Two-Dimensional Theranostic Nanomaterials in Cancer

Subjects: Oncology | Materials Science, Biomaterials | Biotechnology & Applied Microbiology
Contributor: Dong-Wook Han

As the combination of therapies enhances the performance of biocompatible materials in cancer treatment, theranostic therapies are attracting increasing attention rather than individual approaches.

Keywords: two-dimensional nanomaterials ; cancer theranostics ; tumor ; biomedical imaging ; in vitro and in vivo biological applications

1. Two-Dimensional Theranostic Nanomaterials

The term "theranostic" refers to a comprehensive effort that integrates diagnostics and therapy in a single nanoplatform [1][2]. Nanotheranostic harnesses the capabilities of nanotechnology, enhancing therapeutic efficacy and diagnosing ability with a marked difference compared to other currently available diagnoses and therapies, including chemotherapy [3], immunotherapy [4] and radiotherapy [5]. Though numerous classes of theranostic nanomaterials have been developed for cancer treatment, two-dimensional (2D) nanomaterials and their nanocomposites have been reported to exhibit remarkable advantages in cancer diagnosis and therapy owing to their ultrathin planar nanostructure and intriguing physiochemical properties. The ultrahigh specific surface area rendered by the large lateral size and ultrathin thickness, electron confinement without interlayer interactions, and maximum mechanical flexibility are unique properties of 2D nanomaterials, which differentiate them from their bulk counterparts and other types of nanomaterials such as zero-, one-, and three-dimensional networks [6]. The ultrathin planar nanostructure of these 2D bio-nanosystems provides numerous anchoring sites for therapeutic drug molecules.

Among these 2D nanomaterials, MXene [7][8], transition metal dichalcogenide (TMDC) [9][10][11][12][13], black phosphorus (BP) [14][15][16][17], graphene oxide (GO) [18][19][20][21], manganese dioxide (MnO_2) [22][23][24], and palladium (Pd) [25][26][27] have attracted tremendous attention in cancer theranostics [28][29][30]. Generally, 2D inorganic nanoparticles are synthesized either by bottom-up or top-down approaches. The bottom-up methods include organic ligand-assisted growth, 2D template-confined growth, seeded growth, small molecules and ions mediated synthesis, hydro-/solvothermal methods, crystal phase transformation, biological synthesis, and nanoparticle assembly. Mechanical compression, exfoliation, and nanolithography are the methods of top-down approaches [31].

MXenes, which denote the family of 2D transition metal carbides, carbonitrides, and nitrides, have emerged as potential nanocarriers with the intrinsic property of photothermal-conversion in cancer hyperthermia. The temperature point in the surrounding of MXene is elevated upon external irradiation by a near-infrared (NIR) laser with an excitation wavelength at 808 nm. It has been reported that cancerous cells are more sensitive to heat than normal healthy cells. In this context, MXenes have proved capable candidates in the field of biomedicine. Generally, MXenes are produced by extracting A-element from the layered ternary carbides of MAX phases. M indicates an early transition metal, whereas A denotes an A group element in the periodic table. X can be either C or N. There are reports that MXenes exhibit excellent hydrophilicity, metallic conductivity, and mechanical properties [32][33]. It was reported that MXenes, including Ti_3C_2Tx and Nb_2CTx produced by a solvothermal treatment, had five times greater surface areas than the MXenes generated by a HF-etching protocol [34]. In 2016, the first nitride MXene was reported, priduced by the reaction of the MAX phase precursor with molten salts at high temperatures [35]. Limbu et al. described a facile and environmentally benign reduced Ti_3C_2Tx MXene prepared through a simple treatment with L-ascorbic acid at room temperature [36]. TMDCs, including MoS_2, $MoSe_2$, WS_2, WSe_2, and Bi_2Se_3, consist of hexagonal layers of metal atoms sandwiched between two layers of chalcogen atoms. Several research groups have explored TMDCs as drug delivery platforms and NIR-absorbing agents for cancer combination therapy [37]. Many methods, such as direct solvothermal synthesis, chemical vapor deposition, mechanical and chemical exfoliation, and thermal ablation, have been adopted for the scaled-up production of TMDC nanosheets [38]. TMDCs such as NbS_2, MoS_2, and WS_2 were synthesized by the vapor-phase reaction of their respective metal chloride salts at 800-850 °C [39]. Yu et al. have demonstrated the mechanism of deposition in TMDC systems by studying the removal of MoS_2 nanosheets from the precursor $MoCl_5$ in the presence of sulfur gas by the low-pressure chemical vapor deposition reaction [40]. They stated that the rate-limiting step is governed by the relative partial pressure of the MoS_2 gas

and the vapor pressure of the growing MoS_2 NSs. It was proved that mono-, bi- and tri-layer MoS_2 nanosheets could be generated if the oxygen plasma treatment is controlled with durations of 90, 120, and 300 s, respectively, prior to its growth [41].

Due to the large surface area by volume and intrinsic high NIR absorbance, nanographene oxide (NGO) nanosheets act as the carrier for photosensitizers and photothermal agents as well [42]. They can load many water-insoluble drugs with π–π hydrophobic interactions. They display remarkable theranostic behavior in combinatorial photodynamic and photothermal (PDT/PTT) treatment under 808 nm laser irradiation and hence have been widely used in cancer treatment [43]. It has also been reported that the mass extinction coefficient of GOs is relatively larger than that of gold nanorods. Owing to the fact they are economically inexpensive, GOs have found many more applications in nanomedicine and electrical devices than carbon nanotubes [44]. Li et al. obtained either a monolayer or a few layers of graphene NSs from worm-like graphite in 1-methyl-2-pyrrolidinone suspension using a facial liquid phase exfoliation procedure [45]. Ramesha et al. produced reduced graphene oxide by reducing the exfoliated graphene oxide, which had a high surface area lacking a high negative surface charge [46]. Graphene oxide produced by the Hummers method from flake graphite was reported to interrupt the conjugation in the graphene plane and produce oxygen-containing functional groups, including epoxide, hydroxyl, and carbonyl on its surface [47][48]. Exfoliated 2D MnO_2 nanosheets with ultrathin thickness were reported to exhibit ultrasensitive responsibility to the tumor microenvironment and release Mn^{2+} in response to mild acidic conditions. Solid tumors are metabolically different from healthy tissues in many ways. They produce an excessive amount of lactic acid and H_2O_2 due to the upregulated glycolytic metabolism during tumorigenesis [49][50]. Hence, the metabolism and excretion of the MnO_2 nanosheets could be facilitated during the theranostic tumor treatment [51]. Omomo et al. reported the synthesis of exfoliated layered manganese oxide ($H_{0.13}MnO_2{\cdot}H_2O$) dissolved in tetrabutylammonium hydroxide solution following a top-down approach [52]. Kazuya Kai et al. showed for the first time a single-step bottom-up approach to synthesize MnO_2 NSs directly from an aqueous solution of $MnCl_2$ [53].

Being a most stable allotrope of phosphorous, black phosphorous (BP) shows a layer-dependent energy band spanning from a bulk value (0.3 eV) to a monolayer value (2.0 eV). It has been reported that BP nanosheets exhibit a high photothermal conversion efficiency with a significant NIR extinction coefficient. Further, BPNSs are biocompatible as the final degradation products of BP, such as phosphonate and phosphate, are non-toxic [54]. BPNSs possess a large surface area with a folded plane configuration and act as an efficient drug delivery candidate [55]. Owing to their unique optical, electronic, and mechanical properties, BPNSs have found several versatile biomedical applications. As BP NSs generate singlet oxygen species in the entire visible light region, they could be employed for photodynamic therapy [56]. Brent et al. synthesized a few-layered BP NSs for the first time via the liquid exfoliation procedure of BP in N-methyl-2-pyrrolidone [57]. Smith et al. produced BP NSs (>3 μm^2) from red phosphorus directly on a silicon substrate using a chemical vapor deposition method [58]. Because of their strong and well-defined near-infrared (NIR) surface plasma resonance properties and high photothermal stability, palladium (Pd) nanosheets and their nanostructures have been widely used as photo-based theragnostic agents [59]. In 2009, Siril et al. synthesized ultrathin Pd NSs with a thickness of about 2 nm purging carbon monoxide for the first time [60]. The literature reports revealed that the thickness of Pd NSs could be limited to less than 10 atomic layers by the influence of CO [61]. The shape of Pd NSs was extremely stable on exposure to NIR radiation compared to silver and gold nanostructures. Pd NSs, exhibiting a thickness of 2.3 nm and an average edge length of 124 nm, were produced by reducing palladium (II) acetylacetonate in the presence of aqueous ascorbic acid solution [62]. Some other 2D nanomaterials based on boron and gold are available with limited biomedical applications [63][64]. In the present review, we have compiled in vitro and in vivo cancer-treating multifunctional theranostic application of well-explored 2D theranostic nanomaterials. Many reviews have been published, so far, based on 2D theranostic nanomaterials demonstrating various therapies and treatments. They have listed theranostic application of such nanomaterials with respect to biomedical imaging, photothermal conversion efficiency, and dimensional values, including size and thickness of the nanomaterials [65][66][67]. Some literature showed their biological effects randomly either with in vitro or in vivo treatment [68]. In the current review, we have presented the theranostic application of 2D nanomaterials collecting only the piece of literature works, which demonstrate both in vitro and in vivo biological effects.

2. Theranostic Properties of 2D Nanomaterials in Cancer Treatment

The purpose of theranostic therapy is not only enhancing therapeutic effects but also reducing side effects and improving targeting ability. Due to exceptional theranostic photothermal, photodynamic and chemotherapies, 2D theranostic nanomaterials express magnetic resonance, photoacoustic [69], fluorescence [70][71], and upconversion luminescent imaging ability [72][73], and sometimes lead to targeted drug delivery [74] (Figure 1). The roles of 2D nanostructured materials in cancer treatment by both in vitro and in vivo studies are listed in Table 1.

Photothermal therapy (PTT) is an emerging treatment method to eradicate cancer tumors, in which light energy is converted into heat energy by using NIR-absorbing agents [75][76]. The use of NIR light triggers a high temporal and spatial control of local heating, minimizing adverse side effects. Two essential features viz. reduced tissue scattering, and high photothermal-conversion efficiency need to be followed to achieve an effective tumor-tissue ablation during NIR irradiation. NIR light can be further classified into two, i.e. NIR-I and NIR-II bio windows with the wavelength range of 750–1000 nm and 1000–1350 nm, respectively [77]. During NIR-triggered photothermal treatment, local hyperthermia is produced elevating temperature of the tumor microenvironment more than 42 °C, which is enough to ablate the tumor. Also, PTT bears more significant advantages with minimal invasiveness and a high selectivity than conventional cancer treatment strategies, including simple operation [78].

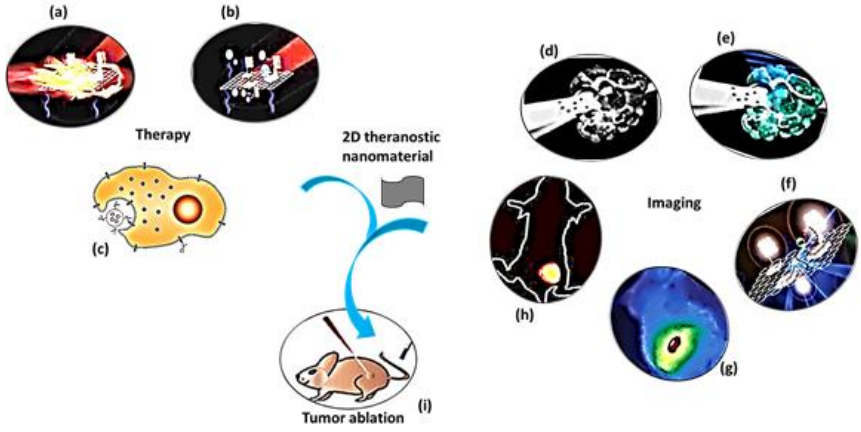

Figure 1. A schematic diagram showing theranostic treatments of 2D theranostic nanomaterials such as photothermal therapy (**a**), photodynamic therapy (**b**) and chemotherapy (**c**) with their astonishing imaging properties, including magnetic resonance (d), photoacoustic (**e**), fluorescence (**f**), infra-red thermal (**g**), and upconversion luminescence imaging (h) to eradicate cancer tumor (**i**) effectively. The images (**a**), (**b**), (**f**), and (**i**) were adapted with permission from [79]. The image (**c**) was adapted with permission from [80]. The images (d) and (**e**) were adapted with permission from [81]. The image (**g**) was adapted with permission from [37]. The image (**h**) was adapted with permission from [82]

Photodynamic therapy (PDT) is an alternative high-efficient cancer treatment approach, which generates a large amount of singlet oxygen ($^1O_2$) from activatable photosensitizers (PS) and subsequently causes apoptosis or necrosis of cells [83][84][85]. Though PTT and PDT therapies are efficient in cancer treatment, some drawbacks are encountered. PTT, sometimes, causes non-specific cellular damage to healthy tissues because a few portions of NIR laser light travel into some healthy tissues while treating tumor tissues. Likewise, the therapeutic effects of PDT are also limited due to the insufficient oxygen supply and limited penetration depth of visible or ultraviolet light sources. In such circumstances, the impact on tumor growth of a single treatment by either PTT or PDT becomes unsatisfactory. Hence, the researchers introduced the integration of PTT and PDT into one system to improve the therapeutic efficacy of studied nanomaterials. Whenever PSs are administered for the PDT treatment, PSs are retained in tumor tissues at a large quantity because the tumor cells possess an inadequate lymphatic system. In contrast, healthy tissues eliminate them over time. Hence, localized activation by NIR irradiation makes PDT a selective treatment for killing cancer cells. The localized oxidative photodamage triggered by the therapy induces three main mechanisms of cell death at the tumor site. They are apoptosis, necrosis, and autophagy, which are accompanied by the induction of an acute local inflammatory reaction to remove dead cells and restore healthy tissue. PDT is a highly controllable therapy owing to a short-range action of singlet oxygen ($^1O_2$) with a lifetime of ~40 ns [86]. Apart from NIR-mediated PDT, alternative strategies such as X-ray PDT and sonodynamic PDT were also developed by the researchers to treat cancer. Sonodynamic therapy (SDT) could activate a sonosensitizer through the sonoluminescence process, pyrolytic reaction, or acoustic cavitation effects [87]. The advantageous property of SDT over PDT is the higher tissue penetration depth [88]. In contrast to conventional PDT, X-ray PDT is essentially a combination of RT and PDT, the key factors of which include X-ray dose, the concentration of O_2, and the efficiency of the intersystem crossing. X-ray PDT is effective in causing oxidative degradation of unsaturated lipids and surface proteins, short-term cell necrosis, and DNA damage [89][90][91][92][93][94].

Tumor imaging technologies, including magnetic resonance (MR) imaging and photoacoustic (PA) imaging, are related to theranostic therapies, which are helpful for the accurate diagnosis of cancer. MR images are clear with subtle changes due to their excellent resolving power in soft tissues. In contrast, PA imaging produces sharp contrast tissue images as a non-invasive and non-ionizing biomedical imaging technique. Some researchers combine different imaging methods to achieve accurate and early diagnosis of cancer [78]. As photosensitizers are susceptible to photo-bleaching and self-destruction upon prolonged light exposure, the development of novel PS nanocomplexes without fluorescence quenching is necessary for theranostic treatment approaches [79]. Upconversion luminescence (UCL) imaging for tumor cells has

attracted substantial attention in recent years owing to the unique properties of upconversion nanomaterials, which minimize the background interference from autofluorescence of biosamples and improve tissue penetration. The upconversion method is an anti-Stokes process whereby two or more low-energy photons from NIR light are absorbed to emit higher energy in the visible region [42]. Sophisticated imaging techniques, including computed tomography, positron emission tomography (PET), and X-rays, are inevitable in cancer diagnosis. When the treatment target is not identified, radiotherapy provides required inputs from imaging for planning the treatment [90].

2D theranostic nanomaterials undergo easy surface modification and hence possess a high drug loading capacity for numerous small-molecule anticancer drugs, enzymes, and therapeutic genes. For instance, PEGylated graphene oxide reported by Liu et al. delivered hydrophobic anticancer drug SN38 with therapeutic efficacy than that of FDA-approved SN38 prodrug [91]. The reasons are the specific interactions such as π–π stacking and hydrophobic forces of aromatic ring-containing anticancer drug molecules with the graphene nanosheets. In the acidic environment of cancer tumors, the nanomaterials release the drug molecules due to the protonation effect [92]. Tao et al. conjugated black phosphorus nanosheets with amine-terminated PEG, whereby the loading capacity of DOX was significantly high by 108% w/w. Further, they demonstrated that the interaction between DOX and the black phosphorus could be disrupted by protonation or hyperthermia [15]. The specificity of drug action gains paramount importance in cancer treatment to ensure the minimization of any toxic effects on healthy cells. It was discovered that cancers could be hematologic or solid tumors, and hence different strategies need to be developed for each type of cancer. The distinctive pathophysiological features of tumor tissue are helpful for targeted drug delivery. Tumor-associated antigens (TAAs) such as folate, low-density lipoprotein, and gonadotropin/luteinizing hormone-releasing hormone receptors are the specific proteins, which are highly expressed over the cancer cells [93][94]. When TAAs are conjugated with theranostic 2D nanomaterials, they would apparently enhance tumor therapy, imaging, and drug delivery along with tumor specificity.

References

1. Doughty, A.C.V.; Hoover, A.R.; Layton, E.; Murray, C.K.; Howard, E.W.; Chen, W.R. Nanomaterial applications in photot hermal therapy for cancer. Materials 2019, 12, 779, doi:10.3390/ma12050779.
2. Wong, X.Y.; Sena-Torralba, A.; Álvarez-Diduk, R.; Muthoosamy, K.; Merkoçi, A. Nanomaterials for nanotheranostics: tun ing their properties according to disease needs. ACS Nano 2020, 14, 2585–2627, doi:10.1021/acsnano.9b08133.
3. Huang, C.-Y.; Ju, D.-T.; Chang, C.-F.; Muralidhar Reddy, P.; Velmurugan, B.K. A review on the effects of current chemot herapy drugs and natural agents in treating non-small cell lung cancer. Biomedicine 2017, 7, 23–23, doi:10.1051/bmdc n/2017070423.
4. Esfahani, K.; Roudaia, L.; Buhlaiga, N.; Del Rincon, S.V.; Papneja, N.; Miller, W.H., Jr. A review of cancer immunothera py: from the past, to the present, to the future. Curr. Oncol. 2020, 27, S87–S97, doi:10.3747/co.27.5223.
5. Chen, H.H.W.; Kuo, M.T. Improving radiotherapy in cancer treatment: Promises and challenges. Oncotarget 2017, 8, 62 742–62758, doi:10.18632/oncotarget.18409.
6. Zhang, H. Ultrathin two-dimensional nanomaterials. ACS Nano 2015, 9, 9451–9469, doi:10.1021/acsnano.5b05040.
7. Dai, C.; Chen, Y.; Jing, X.; Xiang, L.; Yang, D.; Lin, H.; Liu, Z.; Han, X.; Wu, R. Two-dimensional tantalum carbide (MXe nes) composite nanosheets for multiple imaging-guided photothermal tumor ablation. ACS Nano 2017, 11, 12696–127 12, doi:10.1021/acsnano.7b07241.
8. Liu, Z.; Lin, H.; Zhao, M.; Dai, C.; Zhang, S.; Peng, W.; Chen, Y. 2D Superparamagnetic tantalum carbide composite m xenes for efficient breast-cancer theranostics. Theranostics 2018, 8, 1648–1664, doi:10.7150/thno.23369.
9. Wang, S.; Chen, Y.; Li, X.; Gao, W.; Zhang, L.; Liu, J.; Zheng, Y.; Chen, H.; Shi, J. Injectable 2D MoS2-integrated drug delivering implant for highly efficient NIR-triggered synergistic tumor hyperthermia. Adv. Mater. 2015, 27, 7117–7122, d oi:10.1002/adma.201503869.
10. Gong, L.; Yan, L.; Zhou, R.; Xie, J.; Wu, W.; Gu, Z. Two-dimensional transition metal dichalcogenide nanomaterials for combination cancer therapy. J. Mater. Chem. B 2017, 5, 1873–1895, doi:10.1039/C7TB00195A.
11. Chou, S.S.; Kaehr, B.; Kim, J.; Foley, B.M.; De, M.; Hopkins, P.E.; Huang, J.; Brinker, C.J.; Dravid, V.P. Chemically exfol iated MoS2 as near-infrared photothermal agents. Angew. Chem. Int. Ed. 2013, 52, 4160–4164, doi:10.1002/anie.2012 09229.
12. Yuwen, L.; Zhou, J.; Zhang, Y.; Zhang, Q.; Shan, J.; Luo, Z.; Weng, L.; Teng, Z.; Wang, L. Aqueous phase preparation of ultrasmall MoSe2 nanodots for efficient photothermal therapy of cancer cells. Nanoscale 2016, 8, 2720–2726, doi:1 0.1039/C5NR08166A.

13. Liu, Q.; Sun, C.; He, Q.; Khalil, A.; Xiang, T.; Liu, D.; Zhou, Y.; Wang, J.; Song, L. Stable metallic 1T-WS2 ultrathin nano sheets as a promising agent for near-infrared photothermal ablation cancer therapy. Nano Res. 2015, 8, 3982–3991, doi:10.1007/s12274-015-0901-0.

14. Yang, X.; Liu, G.; Shi, Y.; Huang, W.; Shao, J.; Dong, X. Nano-black phosphorus for combined cancer phototherapy: recent advances and prospects. Nanotechnology 2018, 29, 222001, doi:10.1088/1361-6528/aab3f0.

15. Tao, W.; Zhu, X.; Yu, X.; Zeng, X.; Xiao, Q.; Zhang, X.; Ji, X.; Wang, X.; Shi, J.; Zhang, H., et al. Black phosphorus nanosheets as a robust delivery platform for cancer theranostics. Adv. Mater. 2017, 29, 1603276, doi:10.1002/adma.201603276.

16. Sun, Z.; Zhao, Y.; Li, Z.; Cui, H.; Zhou, Y.; Li, W.; Tao, W.; Zhang, H.; Wang, H.; Chu, P.K., et al. TiL4-coordinated black phosphorus quantum dots as an efficient contrast agent for in vivo photoacoustic imaging of cancer. Small 2017, 13, doi:10.1002/smll.201602896.

17. Sun, C.; Wen, L.; Zeng, J.; Wang, Y.; Sun, Q.; Deng, L.; Zhao, C.; Li, Z. One-pot solventless preparation of PEGylated black phosphorus nanoparticles for photoacoustic imaging and photothermal therapy of cancer. Biomaterials 2016, 91, 81–89, doi: 10.1016/j.biomaterials.2016.03.022.

18. Bugárová, N.; Špitálsky, Z.; Mičušík, M.; Bodík, M.; Šiffalovič, P.; Koneracká, M.; Závišová, V.; Kubovčíková, M.; Kajanová, I.; Zaťovičová, M., et al. A Multifunctional graphene oxide platform for targeting cancer. Cancers 2019, 11, 753.

19. Cho, Y.; Kim, H.; Choi, Y. A graphene oxide–photosensitizer complex as an enzyme-activatable theranostic agent. Chem. Comm. 2013, 49, 1202–1204, doi:10.1039/C2CC36297J.

20. Kalluru, P.; Vankayala, R.; Chiang, C.-S.; Hwang, K.C. Nano-graphene oxide-mediated in vivo fluorescence imaging and bimodal photodynamic and photothermal destruction of tumors. Biomaterials 2016, 95, 1–10, doi:10.1016/j.biomaterials.2016.04.006.

21. Kim, Y.-K.; Na, H.-K.; Kim, S.; Jang, H.; Chang, S.-J.; Min, D.-H. One-pot synthesis of multifunctional Au@graphene oxide nanocolloid core@shell nanoparticles for raman bioimaging, photothermal, and photodynamic therapy. Small 2015, 11, 2527–2535, doi:10.1002/smll.201402269.

22. Peng, J.; Dong, M.; Ran, B.; Li, W.; Hao, Y.; Yang, Q.; Tan, L.; Shi, K.; Qian, Z. “One-for-all”-type, biodegradable prussian blue/manganese dioxide hybrid nanocrystal for trimodal imaging-guided photothermal therapy and oxygen regulation of breast cancer. ACS Appl. Mater. Interfaces 2017, 9, 13875–13886, doi:10.1021/acsami.7b01365.

23. Chen, Q.; Feng, L.; Liu, J.; Zhu, W.; Dong, Z.; Wu, Y.; Liu, Z. Intelligent Albumin–MnO2 nanoparticles as pH-/H2O2-responsive dissociable nanocarriers to modulate tumor hypoxia for effective combination therapy. Adv. Mater. 2016, 28, 7129–7136, doi:10.1002/adma.201601902.

24. Zhao, Z.; Fan, H.; Zhou, G.; Bai, H.; Liang, H.; Wang, R.; Zhang, X.; Tan, W. Activatable fluorescence/MRI bimodal platform for tumor cell imaging via MnO2 nanosheet–aptamer nanoprobe. J. Am. Chem. Soc. 2014, 136, 11220–11223, doi:10.1021/ja5029364.

25. Shi, S.; Huang, Y.; Chen, X.; Weng, J.; Zheng, N. Optimization of surface coating on small Pd nanosheets for in vivo near-infrared photothermal therapy of tumor. ACS Appl. Mater. Interfaces 2015, 7, 14369–14375, doi:10.1021/acsami.5b03106.

26. Zhao, Z.X.; Huang, Y.Z.; Shi, S.G.; Tang, S.H.; Li, D.H.; Chen, X.L. Cancer therapy improvement with mesoporous silica nanoparticles combining photodynamic and photothermal therapy. Nanotechnology 2014, 25, 285701, doi:10.1088/0957-4484/25/28/285701.

27. Chen, X.; Shi, S.; Wei, J.; Chen, M.; Zheng, N. Two-dimensional Pd-based nanomaterials for bioapplications. Sci. Bull. 2017, 62, 579–588, doi: 10.1016/j.scib.2017.02.012.

28. Han, X.; Huang, J.; Lin, H.; Wang, Z.; Li, P.; Chen, Y. 2D Ultrathin MXene-based drug-delivery nanoplatform for synergistic photothermal ablation and chemotherapy of cancer. Adv. Healthc. Mater. 2018, 7, e1701394, doi:10.1002/adhm.201701394.

29. Wang, H.; Yang, X.; Shao, W.; Chen, S.; Xie, J.; Zhang, X.; Wang, J.; Xie, Y. Ultrathin black phosphorus nanosheets for efficient singlet oxygen generation. J. Am. Chem. Soc. 2015, 137, 11376–11382, doi:10.1021/jacs.5b06025.

30. He, T.; Li, F.; Huang, Y.; Sun, T.; Lin, J.; Huang, P. Chapter 4 - Graphene as 2D Nano-theranostic materials for cancer. In Handbook of Nanomaterials for Cancer Theranostics, Conde, J., Ed. Elsevier: Amsterdam, Netherlands, 2018; doi:10.1016/B978-0-12-813339-2.00004-9

31. Chen, Y.; Fan, Z.; Zhang, Z.; Niu, W.; Li, C.; Yang, N.; Chen, B.; Zhang, H. Two-dimensional metal nanomaterials: synthesis, properties, and applications. Chem. Rev. 2018, 118, 6409–6455, doi:10.1021/acs.chemrev.7b00727.

32. Lin, H.; Gao, S.; Dai, C.; Chen, Y.; Shi, J. A two-dimensional biodegradable niobium carbide (MXene) for photothermal tumor eradication in NIR-I and NIR-II biowindows. J. Am. Chem. Soc. 2017, 139, 16235–16247, doi:10.1021/jacs.7b078

18.

33. Lukatskaya, M.R.; Mashtalir, O.; Ren, C.E.; Dall'Agnese, Y.; Rozier, P.; Taberna, P.L.; Naguib, M.; Simon, P.; Barsoum, M.W.; Gogotsi, Y. Cation intercalation and high volumetric capacitance of two-dimensional titanium carbide. Science 2013, 341, 1502–1505, doi:10.1126/science.1241488.
34. Peng, C.; Wei, P.; Chen, X.; Zhang, Y.; Zhu, F.; Cao, Y.; Wang, H.; Yu, H.; Peng, F. A hydrothermal etching route to synthesis of 2D MXene (Ti3C2, Nb2C): Enhanced exfoliation and improved adsorption performance. Ceram. Int. 2018, 44, 18886–18893, doi: 10.1016/j.ceramint.2018.07.124.
35. Urbankowski, P.; Anasori, B.; Makaryan, T.; Er, D.; Kota, S.; Walsh, P.L.; Zhao, M.; Shenoy, V.B.; Barsoum, M.W.; Gogotsi, Y. Synthesis of two-dimensional titanium nitride Ti4N3 (MXene). Nanoscale 2016, 8, 11385–11391, doi:10.1039/C6NR02253G.
36. Limbu, T.B.; Chitara, B.; Orlando, J.D.; Garcia Cervantes, M.Y.; Kumari, S.; Li, Q.; Tang, Y.; Yan, F. Green synthesis of reduced Ti3C2Tx MXene nanosheets with enhanced conductivity, oxidation stability, and SERS activity. J. Mater. Chem. C 2020, 8, 4722–4731, doi:10.1039/C9TC06984D.
37. Qian, X.; Shen, S.; Liu, T.; Cheng, L.; Liu, Z. Two-dimensional TiS2 nanosheets for in vivo photoacoustic imaging and photothermal cancer therapy. Nanoscale 2015, 7, 6380–6387, doi:10.1039/C5NR00893J.
38. Bai, J.; Jia, X.; Ruan, Y.; Wang, C.; Jiang, X. Photosensitizer-conjugated Bi2Te3 nanosheets as theranostic agent for synergistic photothermal and photodynamic therapy. Inorg. Chem. 2018, 57, 10180–10188, doi:10.1021/acs.inorgchem.8b01385.
39. Brent, J.R.; Savjani, N.; O'Brien, P. Synthetic approaches to two-dimensional transition metal dichalcogenide nanosheets. Prog. Mater. Sci. 2017, 89, 411–478, doi: 10.1016/j.pmatsci.2017.06.002.
40. Yu, Y.; Li, C.; Liu, Y.; Su, L.; Zhang, Y.; Cao, L. Controlled scalable synthesis of uniform, high-quality monolayer and few-layer MoS2 films. Sci. Rep. 2013, 3, 1866, doi:10.1038/srep01866.
41. Jeon, J.; Jang, S.K.; Jeon, S.M.; Yoo, G.; Jang, Y.H.; Park, J.-H.; Lee, S. Layer-controlled CVD growth of large-area two-dimensional MoS2 films. Nanoscale 2015, 7, 1688–1695, doi:10.1039/C4NR04532G.
42. Gulzar, A.; Xu, J.; Yang, D.; Xu, L.; He, F.; Gai, S.; Yang, P. Nano-graphene oxide-UCNPs-Ce6 covalently constructed nanocomposite for NIR-mediated bioimaging and PTT/PDT combinatorial therapy. Dalton Trans. 2018, 47, doi:10.1039/C7DT04141A.
43. Luo, S.; Yang, Z.; Tan, X.; Wang, Y.; Zeng, Y.; Wang, Y.; Li, C.; Li, R.; Shi, C. Multifunctional photosensitizer grafted on polyethylene glycol and polyethylenimine dual-functionalized nanographene oxide for cancer-targeted near-infrared imaging and synergistic phototherapy. ACS Appl. Mater. Interfaces 2016, 8, 17176–17186, doi:10.1021/acsami.6b05383.
44. Kim, H.; Lee, D.; Kim, J.; Kim, T.-i.; Kim, W.J. Photothermally triggered cytosolic drug delivery via endosome disruption using a functionalized reduced graphene oxide. ACS Nano 2013, 7, 6735–6746, doi:10.1021/nn403096s.
45. Li, Y.; Zhang, P.; Du, Q.; Peng, X.; Liu, T.; Wang, Z.; Xia, Y.; Zhang, W.; Wang, K.; Zhu, H., et al. Adsorption of fluoride from aqueous solution by graphene. J. Colloid Interface Sci. 2011, 363, 348–354, doi: 10.1016/j.jcis.2011.07.032.
46. Ramesha, G.K.; Vijaya Kumara, A.; Muralidhara, H.B.; Sampath, S. Graphene and graphene oxide as effective adsorbents toward anionic and cationic dyes. J. Colloid Interface Sci. 2011, 361, 270–277, doi:10.1016/j.jcis.2011.05.050.
47. Lü, K.; Zhao, G.; Wang, X. A brief review of graphene-based material synthesis and its application in environmental pollution management. Chinese Sci. Bull. 2012, 57, 1223–1234, doi:10.1007/s11434-012-4986-5.
48. Hong, S.W.; Lee, J.H.; Kang, S.H.; Hwang, E.Y.; Hwang, Y.-S.; Lee, M.H.; Han, D.-W.; Park, J.-C. Enhanced neural cell adhesion and neurite outgrowth on graphene-based biomimetic substrates. Biomed Res. Int. 2014, 2014, 212149, doi: 10.1155/2014/212149.
49. Cheng, L.; Wang, C.; Liu, Z. Upconversion nanoparticles and their composite nanostructures for biomedical imaging and cancer therapy. Nanoscale 2013, 5, 23–37, doi:10.1039/C2NR32311G.
50. Fan, W.; Bu, W.; Shen, B.; He, Q.; Cui, Z.; Liu, Y.; Zheng, X.; Zhao, K.; Shi, J. Intelligent MnO2 nanosheets anchored with upconversion nanoprobes for concurrent pH-/H2O2-responsive UCL imaging and oxygen-elevated synergetic therapy. Adv. Mater. 2015, 27, 4155–4161, doi:10.1002/adma.201405141.
51. Liu, Z.; Zhang, S.; Lin, H.; Zhao, M.; Yao, H.; Zhang, L.; Peng, W.; Chen, Y. Theranostic 2D ultrathin MnO2 nanosheets with fast responsibility to endogenous tumor microenvironment and exogenous NIR irradiation. Biomaterials 2018, 155, 54–63, doi: 10.1016/j.biomaterials.2017.11.015.
52. Omomo, Y.; Sasaki, T.; Wang; Watanabe, M. Redoxable nanosheet crystallites of MnO2 derived via delamination of a layered manganese oxide. J. Am. Chem. Soc. 2003, 125, 3568–3575, doi:10.1021/ja021364p.

53. Kai, K.; Yoshida, Y.; Kageyama, H.; Saito, G.; Ishigaki, T.; Furukawa, Y.; Kawamata, J. Room-temperature synthesis of manganese oxide monosheets. J. Am. Chem. Soc. 2008, 130, 15938–15943, doi:10.1021/ja804503f.

54. Zeng, X.; Luo, M.; Liu, G.; Wang, X.; Tao, W.; Lin, Y.-X.; Ji, X.; Nie, L.; Mei, L. Polydopamine-modified black phosphorous nanocapsule with enhanced stability and photothermal performance for tumor multimodal treatments. Adv. Sci. 2018, 5, 1800510, doi:10.1002/advs.201800510.

55. Yang, X.; Wang, D.; Zhu, J.; Xue, L.; Ou, C.; Wang, W.; Lu, M.; Song, X.; Dong, X. Functional black phosphorus nanosheets for mitochondria-targeting photothermal/photodynamic synergistic cancer therapy. Chem. Sci. 2019, 10, 3779–3785, doi:10.1039/C8SC04844D.

56. Wang, H.; Zhong, L.; Liu, Y.; Xu, X.; Xing, C.; Wang, M.; Bai, S.-M.; Lu, C.-H.; Yang, H.-H. A black phosphorus nanosheet-based siRNA delivery system for synergistic photothermal and gene therapy. Chem. Commun. 2018, 54, 3142–3145, doi:10.1039/C8CC00931G.

57. Brent, J.R.; Savjani, N.; Lewis, E.A.; Haigh, S.J.; Lewis, D.J.; O'Brien, P. Production of few-layer phosphorene by liquid exfoliation of black phosphorus. Chem. Commun. 2014, 50, 13338–13341, doi:10.1039/C4CC05752J.

58. Smith, J.B.; Hagaman, D.; Ji, H.-F. Growth of 2D black phosphorus film from chemical vapor deposition. Nanotechnology 2016, 27, 215602, doi:10.1088/0957-4484/27/21/215602.

59. Chen, M.; Chen, S.; He, C.; Mo, S.; Wang, X.; Liu, G.; Zheng, N. Safety profile of two-dimensional Pd nanosheets for photothermal therapy and photoacoustic imaging. Nano Res. 2017, 10, 1234–1248, doi:10.1007/s12274-016-1349-6.

60. Siril, P.F.; Ramos, L.; Beaunier, P.; Archirel, P.; Etcheberry, A.; Remita, H. Synthesis of ultrathin hexagonal palladium nanosheets. Chem. Mater. 2009, 21, 5170–5175, doi:10.1021/cm9021134.

61. Huang, X.; Tang, S.; Mu, X.; Dai, Y.; Chen, G.; Zhou, Z.; Ruan, F.; Yang, Z.; Zheng, N. Freestanding palladium nanosheets with plasmonic and catalytic properties. Nat. Nanotechnol. 2011, 6, 28–32, doi:10.1038/nnano.2010.235.

62. Zhang, Y.; Wang, M.; Zhu, E.; Zheng, Y.; Huang, Y.; Huang, X. Seedless growth of palladium nanocrystals with tunable structures: from tetrahedra to nanosheets. Nano Lett. 2015, 15, 7519–7525, doi:10.1021/acs.nanolett.5b04019.

63. Wu, C.-Y.; Lin, J.-J.; Chang, W.-Y.; Hsieh, C.-Y.; Wu, C.-C.; Chen, H.-S.; Hsu, H.-J.; Yang, A.-S.; Hsu, M.-H.; Kuo, W.-Y. Development of theranostic active-targeting boron-containing gold nanoparticles for boron neutron capture therapy (BNCT). Colloids Surf. B 2019, 183, 110387, doi:10.1016/j.colsurfb.2019.110387.

64. Guo, J.; Rahme, K.; He, Y.; Li, L.-L.; Holmes, J.D.; O'Driscoll, C.M. Gold nanoparticles enlighten the future of cancer theranostics. Int. J. Nanomed. 2017, 12, 6131–6152, doi:10.2147/IJN.S140772.

65. Murugan, C.; Sharma, V.; Murugan, R.K.; Malaimegu, G.; Sundaramurthy, A. Two-dimensional cancer theranostic nanomaterials: Synthesis, surface functionalization and applications in photothermal therapy. J. Control. Release 2019, 299, 1–20, doi:10.1016/j.jconrel.2019.02.015.

66. Wang, X.; Cheng, L. Multifunctional two-dimensional nanocomposites for photothermal-based combined cancer therapy. Nanoscale 2019, 11, 15685–15708, doi:10.1039/C9NR04044G.

67. Wang, J.; Yang, M. 11 - Two-dimensional nanomaterials in cancer theranostics. In Theranostic Bionanomaterials, Cui, W., Zhao, X., Eds. Elsevier: Amsterdam, Netherlands, 2019; doi:10.1016/B978-0-12-815341-3.00011-0

68. Mohammadpour, Z.; Majidzadeh-A, K. Applications of Two-dimensional nanomaterials in breast cancer theranostics. ACS Biomater. Sci. Eng. 2020, 6, 1852–1873, doi:10.1021/acsbiomaterials.9b01894.

69. Wang, L.V.; Hu, S. Photoacoustic tomography: in vivo imaging from organelles to organs. Science 2012, 335, 1458, doi:10.1126/science.1216210.

70. Yan, W.; Wang, X.-H.; Yu, J.; Meng, X.; Qiao, P.; Yin, H.; Zhang, Y.; Wang, P. Precise and label-free tumour cell recognition based on a black phosphorus nanoquenching platform. J. Mater. Chem. B 2018, 6, 5613–5620, doi:10.1039/C8TB01275J.

71. Liu, H.; Tian, T.; Ji, D.; Ren, N.; Ge, S.; Yan, M.; Yu, J. A Graphene-enhanced imaging of microRNA with enzyme-free signal amplification of catalyzed hairpin assembly in living cells. Biosens. Bioelectron. 2016, 85, 909–914, doi:10.1016/j.bios.2016.06.015.

72. Dibaba, S.T.; Wei, R.; Xi, W.; Zhao, L.; Shi, L.; Ren, W.; Mayr, T.; Sun, L. Theranostic nanocomposite from upconversion luminescent nanoparticles and black phosphorus nanosheets. RSC Advances 2018, 8, 35706–35718, doi:10.1039/C8RA07441K.

73. Wang, C.; Cheng, L.; Liu, Z. Upconversion nanoparticles for photodynamic therapy and other cancer therapeutics. Theranostics 2013, 3, 317–330, doi:10.7150/thno.5284.

74. Hwang, D.W.; Kim, H.Y.; Li, F.; Park, J.Y.; Kim, D.; Park, J.H.; Han, H.S.; Byun, J.W.; Lee, Y.S.; Jeong, J.M., et al. In vivo visualization of endogenous miR-21 using hyaluronic acid-coated graphene oxide for targeted cancer therapy. Biomat

erials 2017, 121, 144–154, doi:10.1016/j.biomaterials.2016.12.028.

75. Mármol, I.; Quero, J.; Rodríguez-Yoldi, M.J.; Cerrada, E. Gold as a possible alternative to platinum-based chemotherap y for colon cancer treatment. Cancers 2019, 11, 780.
76. Kim, M.; Kim, G.; Kim, D.; Yoo, J.; Kim, D.-K.; Kim, H. Numerical study on effective conditions for the induction of apopt otic temperatures for various tumor aspect ratios using a single continuous-wave laser in photothermal therapy using g old nanorods. Cancers 2019, 11, 764.
77. Lin, H.; Wang, X.; Yu, L.; Chen, Y.; Shi, J. Two-dimensional ultrathin MXene ceramic nanosheets for photothermal conv ersion. Nano Lett. 2017, 17, 384–391, doi:10.1021/acs.nanolett.6b04339.
78. Pan, J.; Zhu, X.; Chen, X.; Zhao, Y.; Liu, J. Gd3+-doped MoSe2 nanosheets used as a theranostic agent for bimodal im aging and highly efficient photothermal cancer therapy. Biomater. Sci. 2018, 6, 372–387, doi:10.1039/c7bm00894e.
79. Yan, X.; Hu, H.; Lin, J.; Jin, A.J.; Niu, G.; Zhang, S.; Huang, P.; Shen, B.; Chen, X. Optical and photoacoustic dual-mod ality imaging guided synergistic photodynamic/photothermal therapies. Nanoscale 2015, 7, 2520–2526, doi:10.1039/c4 nr06868h.
80. Kutova, O.M.; Guryev, E.L.; Sokolova, E.A.; Alzeibak, R.; Balalaeva, I.V. Targeted delivery to tumors: multidirectional str ategies to improve treatment efficiency. Cancers 2019, 11, 68, doi:10.3390/cancers11010068.
81. Dai, C.; Lin, H.; Xu, G.; Liu, Z.; Wu, R.; Chen, Y. Biocompatible 2D titanium carbide (MXenes) composite nanosheets fo r pH-responsive MRI-guided tumor hyperthermia. Chem. Mater. 2017, 29, 8637–8652, doi:10.1021/acs.chemmater.7b0 2441.
82. Li, X.; Liu, L.; Fu, Y.; Chen, H.; Abualrejal, M.M.A.; Zhang, H.; Wang, Z.; Zhang, H. Peptide-enhanced tumor accumulati on of upconversion nanoparticles for sensitive upconversion luminescence/magnetic resonance dual-mode bioimaging of colorectal tumors. Acta Biomater. 2020, 104, 167–175, doi:10.1016/j.actbio.2020.01.003.
83. Detty, M.R.; Gibson, S.L.; Wagner, S.J. Current clinical and preclinical photosensitizers for use in photodynamic therap y. J. Med. Chem. 2004, 47, 3897–3915, doi:10.1021/jm040074b.
84. Agostinis, P.; Berg, K.; Cengel, K.A.; Foster, T.H.; Girotti, A.W.; Gollnick, S.O.; Hahn, S.M.; Hamblin, M.R.; Juzeniene, A.; Kessel, D., et al. Photodynamic therapy of cancer: an update. CA Cancer. J. Clin. 2011, 61, 250–281, doi:10.3322/c aac.20114.
85. Henderson, B.W.; Gollnick, S.O.; Snyder, J.W.; Busch, T.M.; Kousis, P.C.; Cheney, R.T.; Morgan, J. Choice of oxygen-c onserving treatment regimen determines the inflammatory response and outcome of photodynamic therapy of tumors. Cancer Res. 2004, 64, 2120–2126, doi:10.1158/0008-5472.can-03-3513.
86. Gazzi, A.; Fusco, L.; Khan, A.; Bedognetti, D.; Zavan, B.; Vitale, F.; Yilmazer, A.; Delogu, L.G. Photodynamic therapy ba sed on graphene and MXene in cancer theranostics. Front. Bioeng. Biotech. 2019, 7, doi:10.3389/fbioe.2019.00295.
87. Wan, G.Y.; Liu, Y.; Chen, B.W.; Liu, Y.Y.; Wang, Y.S.; Zhang, N. Recent advances of sonodynamic therapy in cancer tre atment. Cancer Biol. Med. 2016, 13, 325–338, doi:10.20892/j.issn.2095-3941.2016.0068.
88. Canavese, G.; Ancona, A.; Racca, L.; Canta, M.; Dumontel, B.; Barbaresco, F.; Limongi, T.; Cauda, V. Nanoparticle-assi sted ultrasound: A special focus on sonodynamic therapy against cancer. Chem. Eng. J. 2018, 340, 155–172, doi:10.10 16/j.cej.2018.01.060.
89. Sivasubramanian, M.; Chuang, Y.C.; Lo, L.-W. Evolution of nanoparticle-mediated photodynamic therapy: from superfici al to deep-seated cancers. Molecules 2019, 24, 520, doi:10.3390/molecules24030520.
90. Goyal, S.; Kataria, T. Image guidance in radiation therapy: techniques and applications. Radiol. Res. Pract. 2014, 2014, 705604, doi:10.1155/2014/705604.
91. Liu, Z.; Robinson, J.T.; Sun, X.; Dai, H. PEGylated Nanographene Oxide for Delivery of Water-Insoluble Cancer Drugs. J. Am. Chem. Soc. 2008, 130, 10876–10877, doi:10.1021/ja803688x.
92. Li, M.; Luo, Z.; Zhao, Y. Recent advancements in 2D nanomaterials for cancer therapy. Sci. China Chem. 2018, 61, 121 4–1226, doi:10.1007/s11426-018-9294-9.
93. Vasir, J.K.; Labhasetwar, V. Targeted drug delivery in cancer therapy. Technol. Cancer Res. Treat. 2005, 4, 363–374, d oi:10.1177/153303460500400405.
94. Caldorera-Moore, M.E.; Liechty, W.B.; Peppas, N.A. Responsive theranostic systems: integration of diagnostic imaging agents and responsive controlled release drug delivery carriers. Acc. Chem. Res. 2011, 44, 1061–1070, doi:10.1021/ar 2001777.